Strongly Interacting Fermi Gases with Density Imbalance

J. Kinnunen, L. M. Jensen, and P. Törmä

Nanoscience Center, Department of Physics, P.O. Box 35, FIN-40014, University of Jyväskylä, Finland

(Received 21 December 2005; published 22 March 2006)

We consider density-imbalanced Fermi gases of atoms in the strongly interacting, i.e., unitarity, regime. The Bogoliubov–de Gennes equations for a trapped superfluid are solved. They take into account the finite size of the system, as well as give rise to both phase separation and Fulde-Ferrel-Larkin-Ovchinnikov-type oscillations in the order parameter. We show how radio-frequency spectroscopy reflects the phase separation, and can provide direct evidence of the FFLO-type oscillations via observing the nodes of the order parameter.

DOI: 10.1103/PhysRevLett.96.110403 PACS numbers: 05.30.Fk, 03.75.Ss, 32.80.−t, 74.20.Fg

Bardeen-Cooper-Schrieffer (BCS) pairing is behind various forms of superconductivity and superfluidity. A prerequisite for BCS pairing is the matching of the Fermi energies of the two pairing components (e.g., spin-up and spin-down electrons). In the case of spin-imbalanced (polarized) Fermi energies, nonstandard forms of pairing are predicted, such as Fulde-Ferrel-Larkin-Ovchinnikov (FFLO) pairing [1,2], interior gap superfluidity or breached pairing [3–8], and phase separation [9,10]. These exotic quantum states have relevance to many fields of physics, e.g., superconductors in a magnetic field, neutron-proton pairing in nuclear matter, and color superconductivity in high density QCD; for a recent extensive review see [11]. The newly realized strongly interacting superfluid Fermi gases [12–20] offer a promising playground for the study of pairing and superfluidity with variable initial conditions—also imbalanced Fermi energies. Indeed, the first such experiments have recently been done, showing the disappearance of superfluidity and vortices with increasing spin-density imbalance [21], and phase separation [21,22]. Here we consider theoretically the density-imbalanced Fermi gas in the unitarity regime, discuss the role of finite size effects, and show how phase separation and FFLO-type oscillations appear and can be observed in the rf spectrum of the system.

Atomic Fermi gases are confined in magnetic or optical traps and the harmonic trapping potential causes significant finite size effects. For instance, for the density-imbalanced system, clear phase separation of the majority component, i.e., the component with the most atoms, towards the edges of the trap has been experimentally observed in [21,22]. Theoretically, the finite size can be taken into account by solving the Bogoliubov–de Gennes equations in the trap geometry. This has been done for the density-imbalanced case in the BCS limit (weak coupling limit) in [23–25]. In the opposite limit where the coupling is so strong that dimers are formed and undergo Bose-Einstein condensation, the system has been described by a mean-field treatment of a bosonic condensate interacting with fermions in normal state within the local density approximation [26]. Here we consider the intermediate case, where the interactions are strong, but the pairing is still fermionic in nature. In the ultracold atomic Fermi gases this corresponds to the Feshbach-resonance, or unitarity, regime. This regime was considered both in [21,22], thereby our results provide direct comparison to the experiments.

We use the single-channel mean-field resonance superfluidity Hamiltonian [27,28]

$$H = \sum_\sigma \int d\mathbf{r}\Psi_\sigma^\dagger(\mathbf{r})\left[-\frac{\nabla^2}{2m} + V_{\mathrm{trap}}(r) - \mu_\sigma\right]\Psi_\sigma(\mathbf{r}) - U\int d\mathbf{r}\Psi_\uparrow^\dagger(\mathbf{r})\Psi_\downarrow^\dagger(\mathbf{r})\Psi_\downarrow(\mathbf{r})\Psi_\uparrow(\mathbf{r}), \quad (1)$$

where $V_{\mathrm{trap}} = \frac{1}{2}m\omega_0^2 r^2$ is the spherically symmetric harmonic trapping potential with m the atom mass and ω_0 the trap oscillator frequency, μ_σ is the chemical potential for atoms in hyperfine state σ, and U is the effective interaction strength. This describes a two-component ($\sigma = \uparrow, \downarrow$, now two different hyperfine states of the atom) gas with s-wave contact interactions, where the strength of the interaction is tunable via a Feshbach resonance.

Following the treatment in Ref. [28], we expand the field operators in eigenstates of the harmonic potential

$$\Psi_\sigma(\mathbf{r}) = \sum_{nlm}\psi_{nlm}(\mathbf{r})c_{nlm\sigma} = \sum_{nlm}R_{nl}(r)Y_{lm}(\hat{r})c_{nlm\sigma},$$

where $Y_{lm}(\hat{r})$ are the standard spherical harmonics and the radial part is given by

$$R_{nl}(r) = \sqrt{2}(m\omega_0)^{3/4}\sqrt{\frac{n!}{(n+1+1/2)!}}e^{-\bar{r}^2/2}\bar{r}^l L_n^{l+1/2}(\bar{r}^2),$$

where $\bar{r} = \sqrt{m\omega_0}r$ and $L_n^{l+1/2}$ is the Laguerre polynomial. This gives the Hamiltonian

$$H = \sum_{nlm\sigma}\xi_{nl\sigma}c_{nlm\sigma}^\dagger c_{nlm\sigma} - \frac{U}{2}\sum_{nn'lm\sigma}J_{nn'\sigma}^l c_{nlm\sigma}^\dagger c_{n'lm\sigma} - \sum_{nn'lm}F_{nn'}^l[c_{nlm\uparrow}^\dagger c_{n'l-m\downarrow}^\dagger + \mathrm{H.c.}], \quad (2)$$

where the single-particle energies are $\xi_{nl\sigma} = \hbar\omega_0(2n + l + 3/2) - \mu_\sigma$, the matrix element $F_{nn'}^l \equiv \int_0^\infty dr r^2 \times R_{nl}(r)\tilde{\Delta}(r)R_{n'l}(r)$ corresponds to anomalous term that de-

scribes the Cooper pair field $\Delta(r)$, and $J^l_{nn'\sigma} \equiv \sum_{\sigma' \neq \sigma} \int_0^\infty dr r^2 R_{nl}(r) n_{\sigma'}(r) R_{n'l}(r)$ is the Hartree interaction term. The order parameter is given by

$$\Delta(r) = U \sum_{nn'l} \frac{2l+1}{4\pi} R_{nl}(r) R_{n'l}(r) \langle c_{nl0\downarrow} c_{n'l0\uparrow} \rangle, \qquad (3)$$

and the fermion densities are

$$n_\sigma(r) = \sum_{nn'l} \frac{2l+1}{4\pi} R_{nl}(r) R_{n'l}(r) \langle c^\dagger_{nl0\sigma} c_{n'l0\sigma} \rangle. \qquad (4)$$

These equations are solved self-consistently for fixed atom numbers $N_\uparrow$ and $N_\downarrow$ by varying the corresponding chemical potentials μ_σ. The Hamiltonian (2) is diagonalized using the Bogoliubov transformation and the resulting eigenstates are used to calculate the excitation gap and density profiles from Eqs. (3) and (4). The diagonalization gives rise to positive and negative eigenenergies $E_{nl\sigma}$, and, since in a general setting the particle-hole symmetry is broken, we need to keep all the solutions.

We have solved the excitation gap $\Delta(r)$ and the density profiles $n_\sigma(r)$ at zero temperature for 4570 atoms in the majority component ($N_\uparrow$), while the number of atoms in the minority component ($N_\downarrow$) varies. We also tried finite temperatures, but observed no significant changes to the picture. The parameters have been chosen for ^{6}Li in the unitarity limit with interaction parameter $k_F a = -16$, where the Fermi wave vector is given by $\frac{\hbar^2 k_F^2}{2m} = E_F = \hbar\omega_0 (6N_\uparrow)^{1/3}$. The resulting profiles are shown in Figs. 1 and 3 for several polarizations $P \equiv \frac{N_\uparrow - N_\downarrow}{N_\uparrow + N_\downarrow}$.

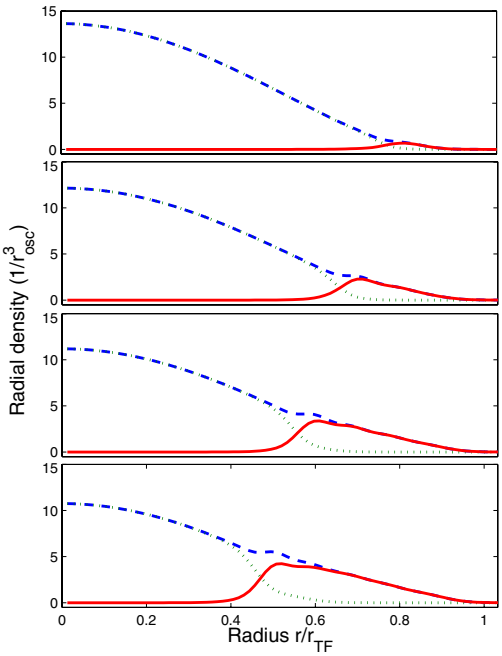

FIG. 1 (color online). The radial density profiles for the majority ($\uparrow$ state, shown in dashed line) and minority ($\downarrow$ state, shown in dotted line) components $n_\sigma(r)$. Solid line shows the density difference as a function of distance from the center of the trap. The polarizations are $P = 0.04$ (upper panel), $P = 0.17$ (upper middle panel), $P = 0.34$ (lower middle panel), and $P = 0.49$ (lower panel).

The main qualitative features of the density profiles in Figs. 1 and 2 agree well with the experiments in Refs. [21,22]. Figure 1 shows the calculated radial density. Experimentally, the densities are observed via imaging from one direction, leading to column integrated densities. Corresponding integrated results from our calculations are shown in Fig. 2. The density profiles show the phase separation into a superfluid core and a normal fluid shell. The core corresponds to equal densities of the two components while at the edges the majority component atoms are dominating. In the column integrated picture Fig. 2, the excess amount of the majority component at the edges of the trap leads to an effective density difference also at $r = 0$. This is seen both in Fig. 2 and in the experiments [21,22]. The bump in the density difference at the edge of the trap is an even more clear signature of phase separation. In [22], two regimes were observed, namely: below polarization $P = 0.1$, a coexistence regime where the density difference does not show clear bumps (actually deviations from Thomas-Fermi profiles were used as the measure), and phase separation regime where these features are clearly visible. According to our results, there is no sharp transition between these two regimes; the phase separation starts immediately even for small polarizations, but the effect then may well be too small to observe. The absence of a sharp transition does not exclude the possibility of a crossover behavior where the amount of phase separation starts to grow faster after a certain threshold. To this extent, we plot in Fig. 4 the excitation gap Δ at center of the trap, as well as the size (volume) of the superfluid

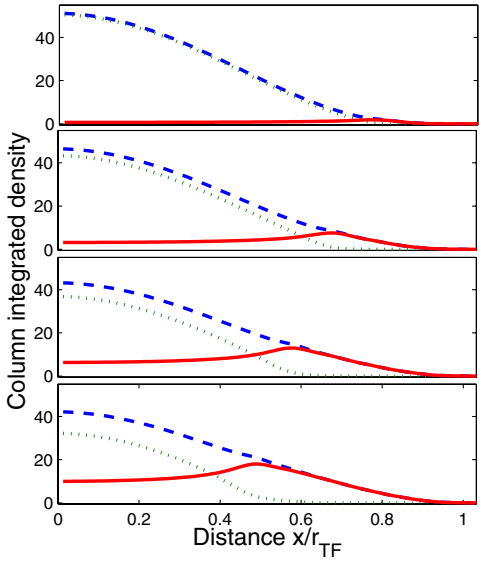

FIG. 2 (color online). The column integrated density profiles for the majority (dashed line) and minority (dotted line) components. Solid line shows the density difference as a function of distance from the center of the trap. The polarizations are the same as in Fig. 1.

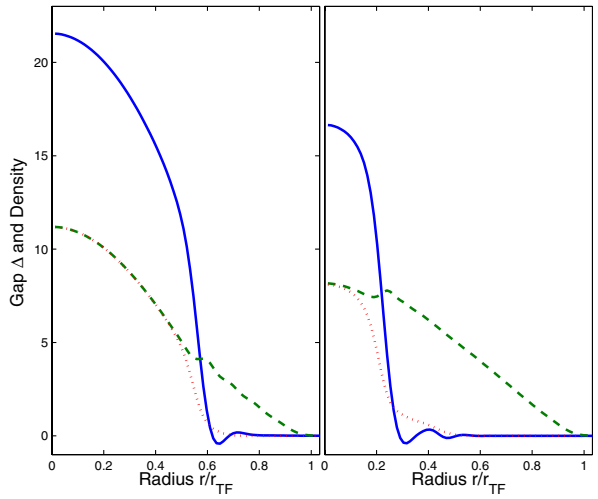

FIG. 3 (color online). The radial density (dashed line for the ↑ state and dotted line for the ↓ state) and the gap (solid line) profiles for polarizations $P = 0.34$ (left) and $P = 0.88$ (right).

core, as functions of the polarization. There might be a change of slopes around the polarization $P = 0.2$, but these results alone are not sufficient for any conclusive statements about a crossover behavior. However, they tell clearly that the value of the gap at the center tends to stay quite constant, and the effect of the polarization is mainly to decrease the superfluid core size. Indeed, the superfluid core size becomes negligible at some polarization P between 0.6–0.9, agreeing well with the experiments [21], where $P = 0.7$ was found to be a threshold for the disappearance of the condensate at the unitarity limit.

In Fig. 5 we show how the phase separation is reflected in the rf spectrum of the gas. rf spectroscopy [29,30] has been used, e.g., to observe the excitation gap of the system [18,31,32]. We calculate the spectra using the method presented in [33]. The results of Fig. 5 show a broad peak at finite rf-field detuning, corresponding to paired

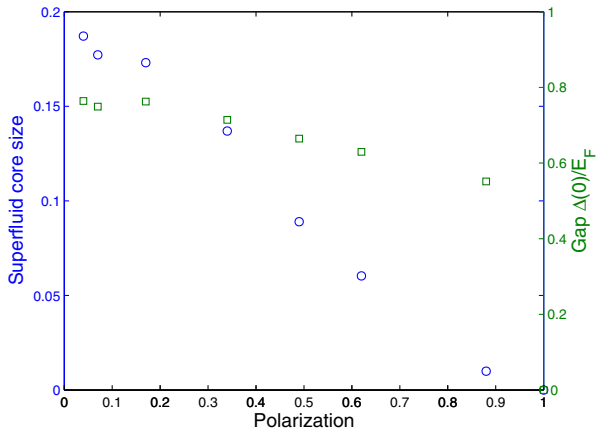

FIG. 4 (color online). The value of the order parameter at the center of the trap (squares) and the fraction of the superfluid core as compared to the Fermi sphere of the major component (circles) plotted as functions of polarization P.

atoms, and the detuning is related to the pairing energy Δ. Note that there are equal amounts of paired atoms for both components. The narrow peak at zero detuning corresponds to the nonpaired majority component atoms at the edge of the trap. This could be a probe of phase separation, complementary to the straightforward observation of the density profiles, since it does not suffer from the effects of column integration and provides a direct comparison between the amounts of the paired and nonpaired atoms.

The gap and density profiles in Fig. 3 show the oscillation of the order parameter and the density as a function of the radial coordinate. Such oscillations have been accounted [23–25] for a FFLO-type phase. The FFLO state in homogenous space leads to oscillations of the order parameter, and is by definition pairing with unequal number of particles. In homogenous space, the FFLO pairing starts only after a critical polarization. In our results, oscillations are also visible for small polarizations, although as tiny effects. This is understandable in the sense that, as the trap favors phase separation, the local polarization at the edges of the trap becomes very easily of considerable size. Therefore, locally one can fulfill the FFLO condition of exceeding a critical polarization, even when the total polarization is small. One could interpret the results in the following way: the trap tends to enforce a normal BCS state at the center of the trap and a FFLO-type state at the edges, and the significance of the latter grows with the total polarization. Is this FFLO-type state observable? It may have existed in the experiments [21,22]. The oscillations of the order parameter are accompanied by oscillations of the densities, and therefore, in principle, one could observe the FFLO characteristics from the density profiles. The column integration, however, tends to wash out the oscillations as can be seen by comparing Figs. 1 and 2. Thus, experimentally it may be difficult

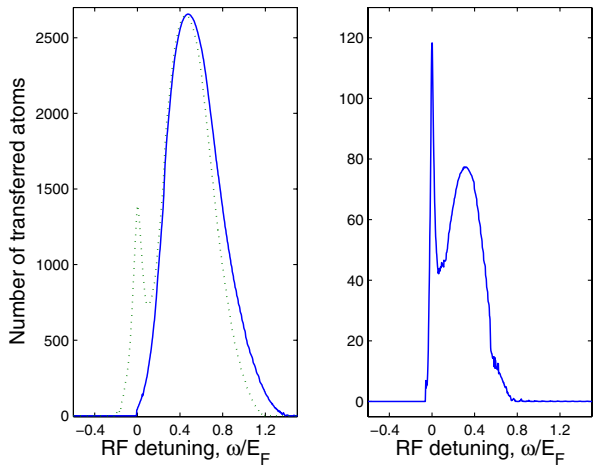

FIG. 5 (color online). The rf spectra for different components. Left panel shows the spectra for both majority (dotted line) and minority (solid line) components for polarization $P = 0.34$, and the right panel shows the spectrum for the minority component for polarization $P = 0.88$. The calculations are done at $T = 0$.

(although column integration can in principle be avoided by more advanced techniques) to detect the FFLO phase from the density profiles. The nodes of the order parameter, however, should be visible in the rf spectrum of the minority component; they produce a peak at zero detuning, reflecting a finite number of nonpaired atoms also in the minority component. This too, may be a small effect for some parameters, e.g., in the left panel of Fig. 4 such a zero detuning peak is not visible in the minority component. However, for parameter values that also produce a more prominent oscillation of the order parameter (Fig. 3 right panel), the zero detuning peak becomes clearly visible, see the right panel in Fig. 4. This is a direct evidence for the nodes of the order parameter. Situations where such signatures are large enough to be observed can probably be achieved experimentally. For instance, we were restricted to spherical geometry due to computational reasons, but a cigar-shaped system is likely to display more prominent oscillations.

In summary, we considered trapped, strongly interacting Fermi gases with unequal populations of the pairing components. We relate our findings to recent experiments and suggest new ways of observing the phase separation and, especially, FFLO features. The system seems to be suited for detailed studies of exotic forms of fermion pairing. Our results show that the trapping potential affects the system in an essential way; spatial regions with different pairing characteristics tend to form and finite size effects have to be carefully taken into account in understanding the system.

This project was supported by Academy of Finland and EUROHORCs (EURYI, Academy Projects No. 106299, No. 205470), and the QUPRODIS project of the EU.

[1] P. Fulde and R. A. Ferrel, Phys. Rev. **135**, A550 (1964).
[2] A. I. Larkin and Y. N. Ovchinnikov, Sov. Phys. JETP **20**, 762 (1965).
[3] G. Sarma, J. Phys. Chem. Solids **24**, 1029 (1963).
[4] R. Combescot, Europhys. Lett. **55**, 150 (2001).
[5] W. V. Liu and F. Wilczek, Phys. Rev. Lett. **90**, 047002 (2003).
[6] B. Deb, A. Mishra, H. Mishra, and P. K. Panigrahi, Phys. Rev. A **70**, 011604 (2004).
[7] E. Gubankova, W. V. Liu, and F. Wilczek, Phys. Rev. Lett. **91**, 032001 (2003).
[8] J. Liao and P. Zhuang, Phys. Rev. D **68**, 114016 (2003).
[9] P. F. Bedaque, H. Caldas, and G. Rupak, Phys. Rev. Lett. **91**, 247002 (2003).
[10] D. E. Sheehy and L. Radzihovsky, Phys. Rev. Lett. **96**, 060401 (2006).
[11] R. Casalbuoni and G. Nardulli, Rev. Mod. Phys. **76**, 263 (2004).
[12] S. Jochim, M. Bartenstein, A. Altmeyer, G. Hendl, C. Chin, J. H. Denschlag, and R. Grimm, Science **302**, 2101 (2003).
[13] M. Greiner, C. A. Regal, and D. S. Jin, Nature (London) **426**, 537 (2003).
[14] C. A. Regal, M. Greiner, and D. S. Jin, Phys. Rev. Lett. **92**, 040403 (2004).
[15] M. W. Zwierlein, C. A. Stan, C. H. Schunck, S. M. F. Raupach, A. J. Kerman, and W. Ketterle, Phys. Rev. Lett. **92**, 120403 (2004).
[16] M. Bartenstein, A. Altmeyer, S. Riedl, S. Jochim, C. Chin, J. H. Denschlag, and R. Grimm, Phys. Rev. Lett. **92**, 203201 (2004).
[17] J. Kinast, S. L. Hemmer, M. E. Gehm, A. Turlapov, and J. E. Thomas, Phys. Rev. Lett. **92**, 150402 (2004).
[18] C. Chin, M. Bartenstein, A. Altmeyer, S. Riedl, S. Jochima, J. Denschlag, and R. Grimm, Science **305**, 1128 (2004).
[19] J. Kinast, A. Turlapov, J. E. Thomas, Q. J. Chen, J. Stajic, and K. Levin, Science **307**, 1296 (2005).
[20] M. W. Zwierlein, J. R. Abo-Shaeer, A. Schirotzek, C. H. Schunck, and W. Ketterle, Nature (London) **435**, 1047 (2005).
[21] M. W. Zwierlein, A. Schirotzek, C. H. Schunck, and W. Ketterle, Science **311**, 492 (2006).
[22] G. B. Partridge, W. Li, R. I. Kamar, Y. an Liao, and R. G. Hulet, Science **311**, 503 (2006).
[23] P. Castorina, M. Grasso, M. Oertel, M. Urban, and D. Zappala, Phys. Rev. A **72**, 025601 (2005).
[24] T. Mizushima, K. Machida, and M. Ichioka, Phys. Rev. Lett. **94**, 060404 (2005).
[25] K. Yang, Phys. Rev. Lett. **95**, 218903 (2005).
[26] P. Pieri and G. C. Strinati, cond-mat/0512354.
[27] G. Bruun, Y. Castin, R. Dum, and K. Burnett, Eur. Phys. J. D **7**, 433 (1999).
[28] Y. Ohashi and A. Griffin, Phys. Rev. A **72**, 013601 (2005).
[29] S. Gupta, Z. Hadzibabic, M. W. Zwierlein, C. A. Stan, K. Dieckmann, C. H. Schunck, E. G. M. van Kempen, B. J. Verhaar, and W. Ketterle, Science **300**, 1723 (2003).
[30] C. A. Regal and D. S. Jin, Phys. Rev. Lett. **90**, 230404 (2003).
[31] P. Törmä and P. Zoller, Phys. Rev. Lett. **85**, 487 (2000).
[32] J. Kinnunen, M. Rodríguez, and P. Törmä, Science **305**, 1131 (2004).
[33] J. Kinnunen and P. Törmä, Phys. Rev. Lett. **96**, 070402 (2006).